Available online at www.sciencedirect.com
ScienceDirect
Scripta Materialia 65 (2011) 25–28
Scripta MATERIALIA
www.elsevier.com/locate/scriptamat

Porous stainless steel hollow fibers with shrinkage-controlled small radial dimensions

Mieke W.J. Luiten-Olieman,[a,*] Michiel J.T. Raaijmakers,[a] Louis Winnubst,[a] Matthias Wessling,[b] Arian Nijmeijer[a] and Nieck E. Benes[a]

[a] *Inorganic Membranes, Department of Science and Technology and MESA+ Institute for Nanotechnology, University of Twente, P.O. Box 217, 7500 AE Enschede, The Netherlands*
[b] *Chemical Process Engineering, RWTH Aachen University, Turmstrasse 46, 52064 Aachen, Germany*

Received 28 February 2011; revised 15 March 2011; accepted 16 March 2011
Available online 23 March 2011

A method is presented for the preparation of thin (~250 μm) porous stainless steel hollow fiber membranes based on dry–wet spinning of a particle-loaded polymer solution followed by heat treatment. Extraordinarily small radial dimensions were achieved by controlled shrinkage during thermal treatment. Above the glass transition temperature of the polymer, the dynamics of surface energy-driven viscous flow allow regulated reduction of the macrovoid volume, resulting in a substantial decrease in the final fiber diameter.

Keywords: Porous stainless steel; Hollow fiber; Metal membrane; Phase separation; Controlled shrinkage

Hollow fiber membranes with small radial dimensions allow a very high surface-area-to-volume ratio, up to $\sim 10^4\ m^{-1}$, and can sustain large hydrostatic pressures. Polymeric hollow fiber membranes are widely used in various biomedical, medical and industrial applications [1,2]. These fibers are made in large quantities via the dry–wet spinning process, in which a polymer solution is pressed through a spinneret and coagulated in a bath of non-solvent [3–6]. As an example of how well established this process is, millions of membrane modules are produced annually for hemodialysis, each containing approximately 1 km of hollow fiber that has a distinct separation performance and no defects [1,2]. On average, these modules typically cost $10–20 each. Inorganic membranes can offer an interesting alternative for applications in which polymers have limited chemical or thermal stability. Currently, no commercial inorganic hollow fiber membranes exist. In the scientific literature, there are reports of porous ceramic hollow fibers that have been made via dry–wet spinning of a polymer solution containing inorganic particles, followed by heat treatment to burn out the polymer and sinter the particles together [7–12]. The applicability of these fibers is hampered by their limited mechanical strength. Recently, metal fibers have been reported that have superior mechanical properties and allow welding and brazing [13]. All of these inorganic porous hollow fibers are relatively thick (~1 mm) in comparison to state-of-the-art polymeric hollow fibers.

Here, we present a method that allows the preparation of stainless steel hollow fibers with an outer diameter that can be regulated down to ~250 μm, comparable to that of typical polymeric hemodialysis and gas separation membranes [2]. The extraordinarily small radial dimensions are achieved by controlled shrinkage of the green fibers at temperatures exceeding the glass transition temperature. At these temperatures, the dynamics of viscous deformation of the green fibers allow regulated reduction of the macrovoid volume and a substantial decrease in the final fiber diameter. The pronounced changes in fiber morphology upon heat treatment are in contrast to observations reported for other inorganic hollow fiber membranes.

Green hollow fibers were prepared via the dry–wet spinning process based on the principle of phase separation; this process has been described in detail elsewhere [13]. Spinning experiments were performed with a spinneret with inner and outer diameters of 0.5 and 1.1 mm, respectively. Deionized water was used as the

* Corresponding author. Tel.: +31 53 4892914; fax: +31 53 489 4611; e-mail: m.w.j.luiten@utwente.nl

1359-6462/$ - see front matter © 2011 Acta Materialia Inc. Published by Elsevier Ltd. All rights reserved.
doi:10.1016/j.scriptamat.2011.03.023

non-solvent in the coagulation bath and as the bore liquid. Spinning mixtures were made by adding stainless steel powder (316L, particle size 4.17 μm according to the manufacturer, Epson Atmix Corporation) to *N*-methylpyrrolidone (NMP, 99.5 wt.%, Aldrich), followed by stirring for 30 min. Polyethersulfone (PES, 6020P, Ultrason) was added in three steps, each separated by 2 h, and the mixture was then stirred for 16 h. The PES/NMP volume ratio was kept constant (1/4), while the concentration of the stainless steel was varied in the range of 23–62 vol.% (with respect to stainless steel + PES, not including the solvent; this definition of the vol.% of stainless steel relates to the composition of the green fiber and is used throughout the remainder of this work). If necessary, 0–1.2 vol.% polyvinylpyrrolidone (PVP, K95, Aldrich) was added to regulate viscosity, followed by stirring for 16 h. The spinning mixtures were degassed before spinning by applying a vacuum for 30 min and leaving the mixtures for 16 h in dry air. The stainless steel powder and PES were dried before use; all other chemicals were used without further treatment. Directly after spinning, the hollow fibers were kept in a water bath for 24 h day to remove all traces of NMP, followed by drying and stretching (0.5 cm m^{-1}) for 24 h.

The thermal treatment of the fibers involved six sequential steps: the fibers were heated to 200 °C (5 °C min^{-1}), 300 °C (1 °C min^{-1}), 400 °C (5 °C min^{-1}), 600 °C (1 °C min^{-1}) and 1100 °C (5 °C min^{-1}, 30 min dwell), then cooled to ambient temperature (5 °C min^{-1}). The changes in morphology in the range of 200–300 °C were analyzed by heating the fiber to a specified temperature (5 °C min^{-1}), keeping the fiber at this temperature for a specified period and then cooling it to ambient temperature (10 °C min^{-1}).

Figure 1 depicts three porous stainless steel hollow fibers and two commercial membranes for comparison. The variation in diameter of the steel fibers is indicative of the range of radial dimensions that can be covered using a single spinneret with fixed dimensions. The only difference in the preparation of the three fibers is the vol.% loading of stainless steel. Prior to heat treatment, the diameters of the fibers were approximately equal (~850 μm). The dimensional changes became apparent after heat treatment, during which the fibers showed a distinct shrinkage. The extent of the shrinkage was larger when the green fiber contained a lower loading of steel particles. The most pronounced change in diameter was observed with a particle loading of 23 vol.%, where the fiber diameter was reduced to only 34% of the initial value. This thin stainless steel hollow fiber had a diameter similar to that of the polymeric fiber and was 13 times thinner than the alumina capillary. In other studies dealing with inorganic fibers, the observed moderate shrinkage during heat treatment was ascribed to densification and the burnout of the polymer [7–9,14,15]. The reductions in diameter reported here are far more pronounced, and volume balance calculations confirmed that polymer burnout alone could not account for the dimensional changes. Additionally, alterations in fiber morphology likely contribute to the extensive shrinkage.

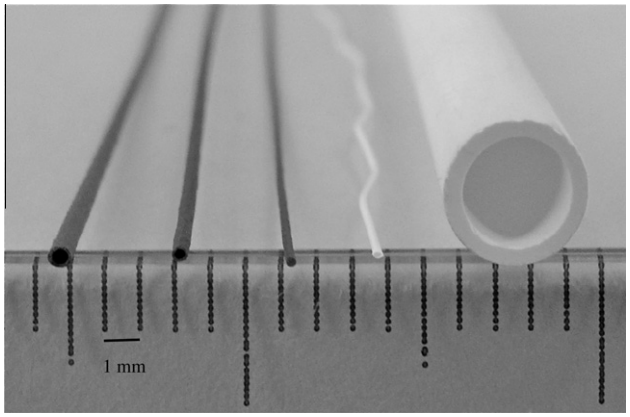

Figure 1. From left to right, three stainless steel hollow fiber membranes with decreasing outer diameters (750, 460 and 285 μm); for comparison, a polymeric (hemodialysis) hollow fiber (060509, Fresenius) and an alumina capillary (M20, Hyflux) are shown.

A series of representative SEM images were selected to illustrate the changes in fiber morphology during heat treatment (see Fig. 2). The fibers on the left are green compacts, whereas those on the right were sintered at 1100 °C. For the fiber with the highest loading of stainless steel particles (Fig. 2A and B, 62 vol.%), the morphology was more or less preserved upon sintering, except for some shrinkage. After sintering, macrovoids were still present in this fiber, similar to what has been observed by others for inorganic hollow fibers with larger diameters [8,9,11,12,16,17]. In contrast, a significant change in the morphology was observed after the sintering of fibers with lower loadings of stainless steel, 41 vol.% (Fig. 2C and D) and 23 vol.% (Fig. 2E and F). Prior to sintering, these fibers possessed distinct macrovoids, but after sintering, these macrovoids disappeared, and a major decrease in outer diameter was observed.

The evolution of fiber length as a function of temperature is depicted in Figure 3. The data clearly show that a predominant part of the shrinkage occurs in the temperature range of 200–300 °C. This temperature range includes the glass transition temperature of polyethersulfone ($T_g = 225$ °C), above which the polymer changes from a glassy to a rubbery material and the mechanical and physical properties change markedly. In particular, the viscoelastic properties of the thermoplastic will vary strongly in this temperature range (see Supporting info). A sufficiently low viscosity of the green fiber can allow for viscous sintering, i.e. surface tension-driven flow under the influence of surface curvature gradients. During viscous sintering, the macrovoid volume in the fibers is reduced, causing a substantial shrinkage of the fiber, as observed for the fibers with loadings of 23, 32 and 41 vol.%. When the particle loading is too high, the viscoelastic properties of the green fibers are dictated by the particles rather than by the polymer, and viscous deformation is obstructed. This finding explains the moderate shrinkage of the fiber with 62 vol.% stainless steel.

The viscous deformation is driven by a reduction in the surface free energy associated with the macrovoids, and the shape and size of these macrovoids are expected to have an influence on the rate of macrovoid decay [18].

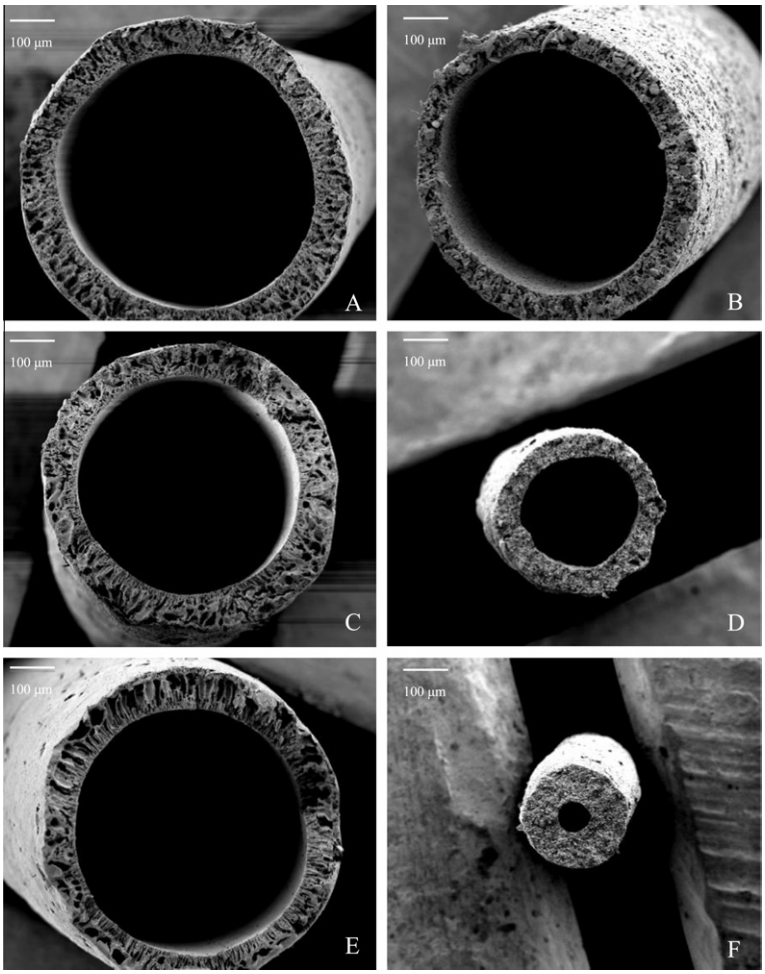

Figure 2. SEM images of hollow fibers with 62, 41 and 23 vol.% stainless steel. Left, green compacts: (A) 62 vol.%, (C) 41 vol.% and (E) 23 vol.%; right, fibers sintered at 1100 °C: (B) 62 vol.%, (D) 41 vol.% and (F) 23 vol.%.

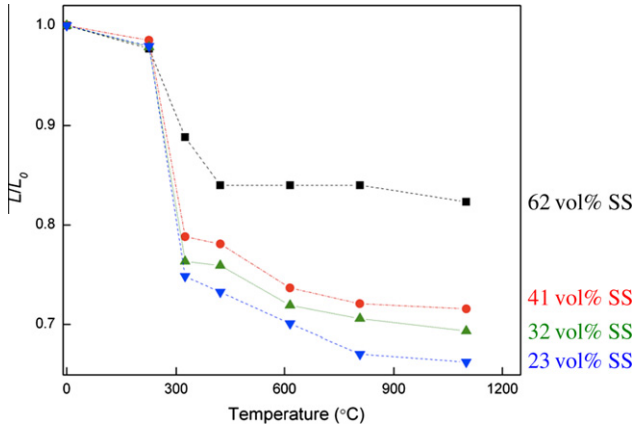

Figure 3. Evolution of fiber length L with temperature for different vol.% stainless steel, normalized with respect to the initial length, L_0.

This effect is illustrated in Figure 4, where the normalized length of the fibers is plotted against time, while the fiber is held at a specified temperature. The data showed that a reduction in length occurred in the first few hours, and the corresponding rate at which the fiber shrank increased with temperature. This result was expected based on the characteristic time for viscous sintering introduced by Kuiken [18], $t_c = l\eta/\sigma$ (where σ is the surface tension and l is the characteristic length), because the dynamic viscosity η decreases with increasing temperature. Within the timescale of the experiment, for each specified temperature, the extent of shrinkage reached an asymptotic value. At lower temperatures, macrovoids disappear only if they are small, whereas for the larger macrovoids, the surface energy driving force is insufficient to overcome the viscous forces. With increasing temperature, viscosity decreases and the decay of larger voids becomes apparent. This behavior was substantiated by the SEM images of fiber cross-sections on the right-hand side of Figure 4. For the fiber incubated at 205 °C, small macrovoids can be identified. After incubation at 225 °C, small macrovoids were no longer visible, but larger macrovoids were still present. The fiber incubated at 245 °C did not exhibit any apparent macrovoids.

Gas permeance was measured, at 21 °C, as a function of pressure difference, up to 7 bar, using a pressure-controlled dead-end gas permeation set-up. Stainless steel hollow fibers (41 vol.%), sintered at 1100 °C, exhibit a nitrogen permeance of $4 \pm 1 \times 10^{-6}$ mol m^{-2} Pa^{-1} s^{-1}.

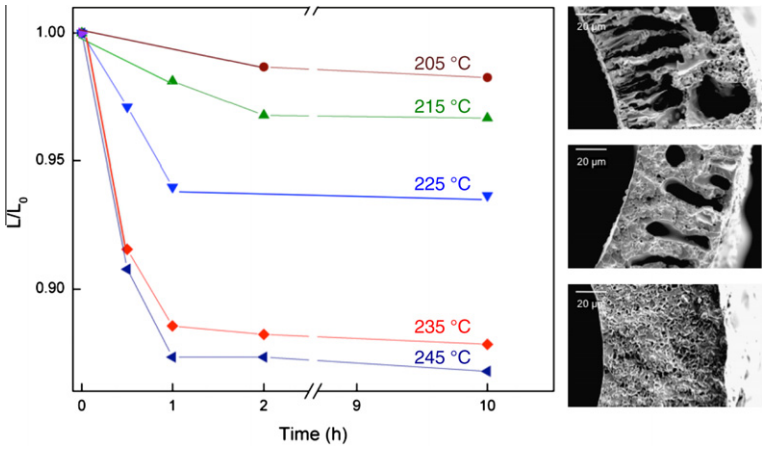

Figure 4. 41 vol.% stainless steel. Left: normalized fiber length as function of time at different temperatures. Right: SEM micrographs of fibers incubated for 10 h at 205, 225, and 245 °C.

In summary, a method was presented for the preparation of porous stainless steel hollow fibers with regulated small radial dimensions by combining a well-established method for the preparation of polymeric hollow fibers with sensible thermal treatment. At ambient temperatures, the morphology of the green fibers, e.g. the degree of macrovoids, can be influenced via the spinning parameters. At temperatures around the glass transition temperature, the shrinkage of the fibers can be controlled; macrovoids with small sizes disappear at lower temperatures, whereas larger macrovoids persist up to higher temperatures. At elevated temperatures (>1000 °C), the pore size distribution of the fibers can be regulated [13]. The method presented here is versatile and generic in nature. Substitution of stainless steel with other particles of different size, shape and composition will allow the manufacture of a broad variety of thin porous inorganic hollow fibers.

Financial support from the Dutch Technology Foundation (STW), within the frame work of project NANOCERFIL (nr 07349), is gratefully acknowledged.

Supplementary data associated with this article can be found, in the online version, at doi:10.1016/j.scriptamat.2011.03.023.

[1] R.W. Baker, Membrane Technology and Applications, 2nd ed., John Wiley & Sons, Chichester, 2008.
[2] I. Moch, Membranes, Hollow-Fiber,Kirk-Othmer Encyclopedia of Chemical Technology, Wiley, 2005.
[3] S. McKelvey, A.D. Clausi, T.W.J. Koros, Journal of Membrane Science 124 (1997) 223.
[4] M. Mulder, Basic Principles of Membrane Technology, 2nd ed., Kluwer Academic Publishers, Dordrecht, 2000.
[5] W.W.Y. Lau, M.D. Guiver, T. Matsuura, Journal of Membrane Science 59 (1991) 8.
[6] H. Strathmann, Desalination 21 (1977) 14.
[7] J. De Jong, N.E. Benes, G.H. Koops, M. Wessling, Journal of Membrane Science 239 (2004) 265.
[8] B. Kingsbury, K. Li, Journal of Membrane Science 328 (2009) 134.
[9] S. Liu, K. Li, R. Hughes, Ceramics International 29 (2003) 875.
[10] T. Van Gestel, D. Sebold, W.A. Meulenberg, M. Bram, H.-P. Buchkremer, Solid State Ionics 179 (2008) 1360.
[11] B. Meng, X. Tan, X. Meng, S. Qiao, S. Liu, Journal of Alloys and Compounds 470 (2009) 461.
[12] S.-M. Lee, I.-H. Choi, S.-W. Myung, J.-Y. Park, I.-C. Kim, W.-N. Kim, K.-H. Lee, Desalination 233 (2008) 32.
[13] M.W.J. Luiten-Olieman, L. Winnubst, M. Wessling, A. Nijmeijer, N.E. Benes, Journal of Membrane Science 370 (2011) 124.
[14] S. Liu, K. Li, Journal of Membrane Science 218 (2003) 269.
[15] X. Tan, S. Liu, K. Li, Journal of Membrane Science 188 (2001) 7.
[16] N. Droushiotis, U. Doraswami, K. Kanawka, G.H. Kelsall, K. Li, Solid State Ionics 180 (2009) 1091.
[17] N. Yang, X. Tan, Z. Ma, Journal of Power Sources 183 (2008) 14.
[18] H.K. Kuiken, Journal of Fluid Mechanics 214 (1990) 13.